Basic dynamic properties of the high-order nonlinear Schrödinger equation

Cangtao Zhou, X. T. He, and Shigang Chen
Center for Nonlinear Studies, Institute of Applied Physics and Computational Mathematics, P.O. Box 8009, Beijing 100088, China
(Received 26 November 1991)

The dynamic behavior of the nonlinear Schrödinger equation (NSE) with an additional high-order Hamiltonian perturbation that displays a nonlinear interaction between Langmuir waves and electrons in plasmas is studied. It is shown that periodic solutions, solitary waves, and recurrence exist, which are also inherent in the cubic NSE. A more important phenomenon, stochasticity, has been found in such a continuum Hamiltonian dynamic system. This phenomenon illustrates that nonintegrability arises from the high-order Hamiltonian perturbation. In addition, our numerical results also show that recurrence, which sensitively depends on initial conditions, is only a special feature of the dynamic system.

PACS number(s): 47.10.+g, 05.45.+b, 52.35.Ra

I. INTRODUCTION

The cubic nonlinear Schrödinger nonlinear equation (NSE)

$$iE_t+E_{xx}+|E|^2E=0 , \tag{1}$$

which is known to be completely integrable by the inverse scattering transform (IST) [1], is one of the basic evolution models for nonlinear waves in various branches of physics. A class of periodic solutions and solitons can be obtained by IST, and much work on Langmuir solitons in plasmas, optical solitons, magnetic solitons, etc., is stimulated [2,3]. The solitons developed by modulational instabilities keep their spatially coherent structures and temporally periodic evolutions.

In particular, it has been found that the unstable modulations to the uniform solution would first grow at an exponential rate as predicted by Benjamin and Feir [4] and that eventually the solution would demodulate and return to a near-uniform state. The energy in the system, which is initially confined to a few low modes, would spread to many higher modes due to the nonlinear interaction, but would eventually regroup into the original modes [5,6]. The well-known Fermi-Pasta-Ulam (FPU) recurrence [7] in connection with deep water waves has been verified experimentally by Lake *et al.* [8] and Yuen and Lake [9]. The simple and complex recurrence phenomena were also discussed numerically by Yuen and Ferguson [10] and analytically by Stiassnie and Korszynski [11].

In recent years, attention has been focused on analyzing the behavior of high-order NSE's involving quintic terms [12–15]. In Langmuir plasmas, the beat-frequency interaction between the large-amplitude parts of high-frequency fields and particles can occur in the evolutive later stages of plasma instability. In Ref. [14], one of us (X.T.H.) derived the dynamic equation involving quintic fields from Vlasov-Maxwell equations. Under the static approximation, the high-order NSE can be written as the following dimensionless form:

$$iE_t+E_{xx}+|E|^2E-g|E|^4E=0 , \tag{2}$$

where $E(X,t)$ is the slowly varying complex amplitude of high-frequency electric fields of plasmons, and g is the coupling constant of high-frequency fields with electrons, which depends on electron temperature and density, etc. The dimensionless density is [15]

$$n(X,t)=-2|E|^2(1-r|E|^2) , \tag{3}$$

where r is taken as

$$r=\begin{cases}3(2T_i+3T_e)/T_e & \text{for Eq. (2)}\\ 0 & \text{for Eq. (1)} .\end{cases} \tag{4}$$

Here T_i and T_e are the temperature of the ion and electron, respectively.

For Eq. (2), a solitary-wave solution was obtained [15] and recurrence was also discussed numerically [12]. It is natural to ask whether periodic solutions can exist and whether integrability will be broken down under high-order Hamiltonian perturbation. To our knowledge, there is no systematic treatment of this problem.

In Sec. II a periodic solution and a solitary wave are obtained. The properties of the solitary wave are discussed from the point of review of physics. The linearized stability analysis is given in Sec. III. The nonintegrable behavior is analyzed in Sec. IV. In Sec. V we simply discuss the relationship of recurrence and stochasticity. Some conclusions are given in the final section.

II. PERIODIC SOLUTION AND SOLITON

Equation (2) can also be derived from the Lagrangian density

$$L=(i/2)(E^*E_t-EE_t^*)-|E_x|^2+\tfrac{1}{2}|E|^4-(g/3)|E|^6 .$$

The invariance of the equation under phase shift, space, and time translations leads to the existence of the following invariants: The quasiparticle number

$$N=\int|E|^2dX , \tag{5}$$

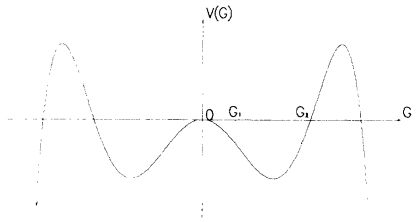

FIG. 1. The pseudopotential function in the regions of $0<g<3/16\alpha^2$.

the momentum

$$P=\tfrac{1}{2}i\int(EE_x^*-E_xE^*)dX\ , \tag{6}$$

and energy

$$H=\int(|E_x|^2-\tfrac{1}{2}|E|^4+\tfrac{1}{3}g|E|^6)dX\ . \tag{7}$$

Defining $E(X,t)=G(X,t)e^{i\Phi(X,t)}$ with G and Φ both real functions, we have equations for G and Φ,

$$G_t+2G_x\Phi_x+G\Phi_{xx}=0\ , \tag{8}$$

$$-G\Phi_t+G_{xx}-G\Phi_x^2+G^3-gG^5=0\ . \tag{9}$$

Also, let

$$G(X,t)=G(\xi),\quad \xi=X-Vt,\quad \Phi=qX-\Omega t\ . \tag{10}$$

Combining Eqs. (8)–(10), we get

$$q=V/2 \tag{11}$$

and

$$\frac{1}{2}\left[\frac{dG}{d\xi}\right]^2+V(G)=H_0\ . \tag{12}$$

Obviously, Eq. (12) is the energy integral of a classical particle with unit mass, H_0 represents the pseudoenergy of a particle, and $V(G)$ is the pseudopotential

$$V(G)=-\tfrac{1}{6}gG^6+\tfrac{1}{4}G^4-\tfrac{1}{2}\alpha^2G^2\ , \tag{13}$$

where $\alpha^2=\frac{1}{4}V^2-\Omega$.

Considering $0<g<3/16\alpha^2$, a plot of the pseudopotential function is given in Fig. 1. A particle lies in the region of pseudoenergy $H_0<0$, and starting from the left point $G=G_1$ will go to the right-hand side of the well, reflect from the place $G=G_2$, and return to $G=G_1$, making a cycle. This particle orbit corresponds to a periodic solution. If a particle lies in the origin point (say $H_0=0$) initially, its orbit corresponds to a very special solution in G, a single-pulse solution called a solitary wave (also called a soliton in an integrable system).

Supposing $H_0\le 0$ and considering

$$\tfrac{1}{3}gG^6-\tfrac{1}{2}G^4+\alpha^2G^2+2H_0=0\ , \tag{14}$$

we can find three positive real roots $G^2=a_1$, a_2, and a_3, and assume $0\le a_1<a_2<a_3$.

Thus, the solution of Eq. (12) can be expressed with the elliptic integrals of the first kind,

$$G(X,t)=\left[\frac{a_2(a_3-a_1)-a_3(a_2-a_1)\mathrm{sn}^2(\sqrt{g/3}M\xi,k)}{(a_3-a_1)-(a_2-a_1)\mathrm{sn}^2(\sqrt{g/3}M\xi,k)}\right]^{1/2}\ , \tag{15}$$

where

$$M=[a_2(a_3-a_1)]^{1/2}\ , \tag{16}$$

$$k=\left[\frac{a_3(a_2-a_1)}{a_2(a_3-a_1)}\right]^{1/2}\ . \tag{17}$$

Hence, the periodic solution of Eq. (2) is

$$E(X,t)=G(X,t)e^{i[(V/2)X-(V^2/4-\alpha^2)t]}\ . \tag{18}$$

If $H_0=0$, we can get

$$a_1=0,\quad a_2=\frac{3[1-(1-\frac{16}{3}g\alpha^2)^{1/2}]}{4g}\ , \tag{19}$$

$$a_3=\frac{3[1+(1-\frac{16}{3}g\alpha^2)^{1/2}]}{4g}$$

and

$$k=1,\quad M=\alpha\sqrt{3/g}\ . \tag{20}$$

Thus, a solitary-wave solution can be obtained

$$E(X,t)=\frac{2\alpha}{[(1-\frac{16}{3}g\alpha^2)^{1/2}\cosh(2\alpha\xi)+1]^{1/2}}\times e^{i[(V/2)X-(V^2/4-\alpha^2)t]}\ . \tag{21}$$

The solitary solution was obtained by Liu and He using the test function method [15]. For Eq. (21), we define $E_0=E(0,0)$ and obtain

$$\alpha^2=\frac{E_0^4}{2}\left[\frac{1}{E_0^2}-\frac{2g}{3}\right]\ ,$$

hence the condition for the soliton wave satisfied is $0\le g<3/2E_0^2$. In the case of $g=0$, the periodic solution for cubic NSE (1) is

$$E(X,t)=\sqrt{2}\alpha\,\mathrm{dn}(\alpha\xi,k)e^{i[(V/2)X-(V^2/4-\alpha^2)t]}\ , \tag{22}$$

and the solitary-wave solution (21) can be reduced to

$$E(X,t)=\sqrt{2}\alpha\,\mathrm{sech}(\alpha\xi)e^{i[(V/2)X-(V^2/4-\alpha^2)t]}\ , \tag{23}$$

which is the so-called Langmuir soliton [16].

The physical significance of the solitary wave is very clear. From Eq. (21), we obtain the height and width of

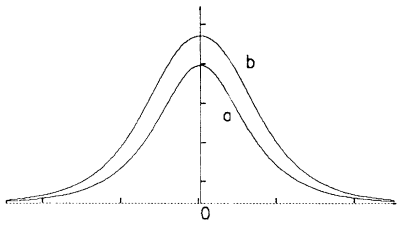

FIG. 2. Solitary-wave solution (21) with $\alpha=1.0$. Curve a corresponds to $g=0$. Curve b corresponds to $g=0.1625$.

the solitary wave,

$$E_{0\max}\approx\sqrt{2}\alpha(1+\tfrac{4}{3}g\alpha^2) , \tag{24}$$

$$\Delta\approx\frac{1}{2\alpha}\ln(17+12\sqrt{2})+\frac{2\sqrt{2}}{3}g\alpha . \tag{25}$$

The pondermotive force creates density depletion, and the maximum density can be obtained from Eq. (3),

$$|n|_{\max}\approx 4\alpha^2[1-(2r-\tfrac{4}{3}g)\alpha^2] . \tag{26}$$

Obviously, the effects of high-order nonlinear terms enhance the amplitude and width of the solitary wave, and weaken the density depletion as compared with those for the case of $g=0$ (see Fig. 2).

III. LINEARIZED STABILITY ANALYSIS

In the preceding section, we only obtain a special periodic solution and a solitary wave. Are there more general periodic solutions and many-solitary solutions? Here, we do not discuss this problem. In this section we further qualitatively analyze the dynamic properties of Eq. (2) and consider the homogeneous solution,

$$E_s(t)=E_0e^{it} , \tag{27}$$

where E_0 are

$$E_0=0 , \qquad E_0=\pm\left[\frac{(1\pm\sqrt{1-4g})}{2g}\right]^{1/2} . \tag{28}$$

The linear growth rate as a function of an unstable wave number K obtained from Eq. (2) is [17]

$$\gamma(K)=K[2E_0^2(1-2gE_0^2)-K^2]^{1/2} \tag{29}$$

for $0<|K|<E_0[2(1-2gE_0^2)]^{1/2}$. The unstable wave number corresponding to the maximum instability mode is $K_{\max}=E_0(1-2gE_0^2)^{1/2}$.

Defining

$$E(X,t)=E_s(t)+\delta E(X,t) \tag{30}$$

and linearizing Eq. (2), we have

$$\begin{bmatrix} i\partial_t+\partial_{xx}+L(|E_0|^2) & h(t) \\ h^*(t) & -i\partial_t+\partial_{xx}+L(|E_0|^2) \end{bmatrix}\begin{bmatrix}\delta E\\ \delta E^*\end{bmatrix}=0 , \tag{31}$$

where L and h are expressed in the following form:

$$L(|E_0|^2)=2|E_0|^2-3g|E_0|^4 , \qquad h(t)=E_s^2(t)(1-2g|E_0|^2) . \tag{32}$$

If we consider the periodic boundary conditions $E(-L/2)=E(L/2)$, the eigenfunction of Eq. (31) can be chosen as

$$\begin{bmatrix}\delta E\\ \delta E^*\end{bmatrix}=\begin{bmatrix}\epsilon e^{i\lambda t}\\ \epsilon^* e^{-i\lambda^* t}\end{bmatrix}\cos(KX) , \tag{33}$$

where ϵ,ϵ^* are small parameters. Here, we choose the wave number of modulational instabilities to the uniform solution as $K=K_{\max}$, and obtain

$$\lambda=1\pm i \tag{34}$$

for cubic NSE (1) as $E_0=\pm1$, and

$$\lambda=1\pm i(-1+4g+\sqrt{1-4g})/2g \tag{35}$$

for high-order NSE (2) as $E_0=\pm[(1-\sqrt{1-4g})/2g]^{1/2}$ with $0\le g<\frac{1}{4}$.

To display the numerical results in later sections, we construct the phase-space diagrams (A,A_t) at $X=0$ as done by Moon [18], which are defined as

$$A(0,t)=|E(0,t)|-E_0 , \qquad A_t(0,t)=\frac{dA(0,t)}{dt} . \tag{36}$$

For phase space (A,A_t), it is easily seen that $E_0=\pm1$ for cubic NSE (1), and

$$E_0=\pm\left[\frac{1-\sqrt{1-4g}}{2g}\right]^{1/2}$$

with $0\le g<\frac{1}{4}$ for Eq. (2) correspond to the hyperbolic fixed points, respectively. The linearized stability analysis also shows that $E_0=0$ for Eqs. (1) and (2) corresponds to the elliptic fixed point. For Eq. (2), the other fixed points, i.e.,

$$E_0=\pm\left[\frac{1+\sqrt{1-4g}}{2g}\right]^{1/2}$$

for all parameter values g, and

$$E_0=\pm\left[\frac{1\pm\sqrt{1-4g}}{2g}\right]^{1/2}$$

for $g>\frac{1}{4}$ correspond to the elliptic points. Because the cubic NSE is integrable, therefore, the trajectories in phase space (A,A_t) correspond to the periodic recurrence solutions. Of course, the different trajectories should be associated with the different initial conditions. The origin is a saddle point.

On the other hand, although the recurrence phenomena have also been found in Eq. (2) [12], the integrable problem has not been discussed. In the following section, we further analyze the integral behavior numerically.

IV. NONINTEGRABILITY

For the cubic NSE (1), the integrability had been corroborated by IST. However, more general NSE's, e.g., higher dimensions or noncubic nonlinearity, do not possess integrability, and many interesting phenomena can appear. For example, a collapse of nonlinear Langmuir waves, when the spatial dimension d and the coefficient p in nonlinear term $|E|^pE$ satisfies $dp>4$, can occur [19]. This important process solves the old problem of small-K condensation in weak turbulent theory. In the case of one dimension, the integrability of systems will, in general, break down if other physical perturbations, such as driven damping [18,20–22], force dissipation [23,25], and nonlinear inhomogeneous media [26,27] are taken into account. A rich variety of temporal chaos and spatial coherence, which suggests that a low-dimensional chaotic attractor exists in an infinite-dimensional system, has been observed [28–31]. In the presence of Hamiltonian perturbations, however, the problem becomes extremely difficult for general initial conditions since the system does not reduce to a finite-dimensional system as that in the case of dissipative perturbations.

In the following discussions, we choose as the initial condition

$$E(X,0)=E_0+0.1e^{i\theta}\cos(K_{\max}X)\ , \tag{37}$$

where

$$E_0=\left[\frac{1-\sqrt{1-4g}}{2g}\right]^{1/2}\ .$$

Obviously, it reduces to the initial conditions as considered by Moon as $g=0$ [18]. In numerical discussions, the periodic boundary conditions and the split-step method [32] have been used. The periodic length is taken as $L=2\pi/K_{\max}$.

According to Eqs. (31)–(35), we obtain

$$\frac{\delta E}{\delta E^*}=\pm i \tag{38}$$

for our dynamic models. Combining Eq. (37), we see that the unstable manifold of the hyperbolic point corresponds to $\theta=45°$ *and* $\theta=225°$ for available values of g. In the case of $g=0$, however, our numerical results show that a homoclinic orbit (HMO) would appear as θ being a bit larger than 45° and the hyperbolic point would deviate from the origin, which results from the modulational amplitude in Eq. (37) being not too small. We find that the period of recurrence for $\theta=45.225°$ is much larger than that for $\theta=0°$ *and* $\theta=90°$ (see Figs. 3 and 6). The trajectory corresponding to $\theta=45.225°$ is near the HMO. In the presence of small perturbation, the periodic trajectories may shift from the HMO to adjacent trajectories whose periods are sensitive to the size of the displacement [24]. The field propagation can then appear to be chaotic. The small perturbation may lead to irregular HMO crossings [18,28].

In numerical experiments, we also find that the phase trajectories for $0°\le\theta<45.225°$ are the periodic motions around an elliptic fixed point and those for $45.225°<\theta\le 90°$ are the periodic motions around two elliptic fixed points and a hyperbolic fixed point, but do not cross over the hyperbolic fixed point. The largest distance for trajectory deviating from the hyperbolic point is that corresponding to $\theta=90°$ [Fig. 6(a)].

Taking $-g|E|^4E$ as a Hamiltonian perturbation, we expect that the irregular motions would easily appear nearby HMO if the integrability of the system is indeed broken down. Figures (4 and 5) clearly illustrate the chaotic behavior of the amplitude of fields. As shown in the figures for the A_t-A phase space, irregular HMO

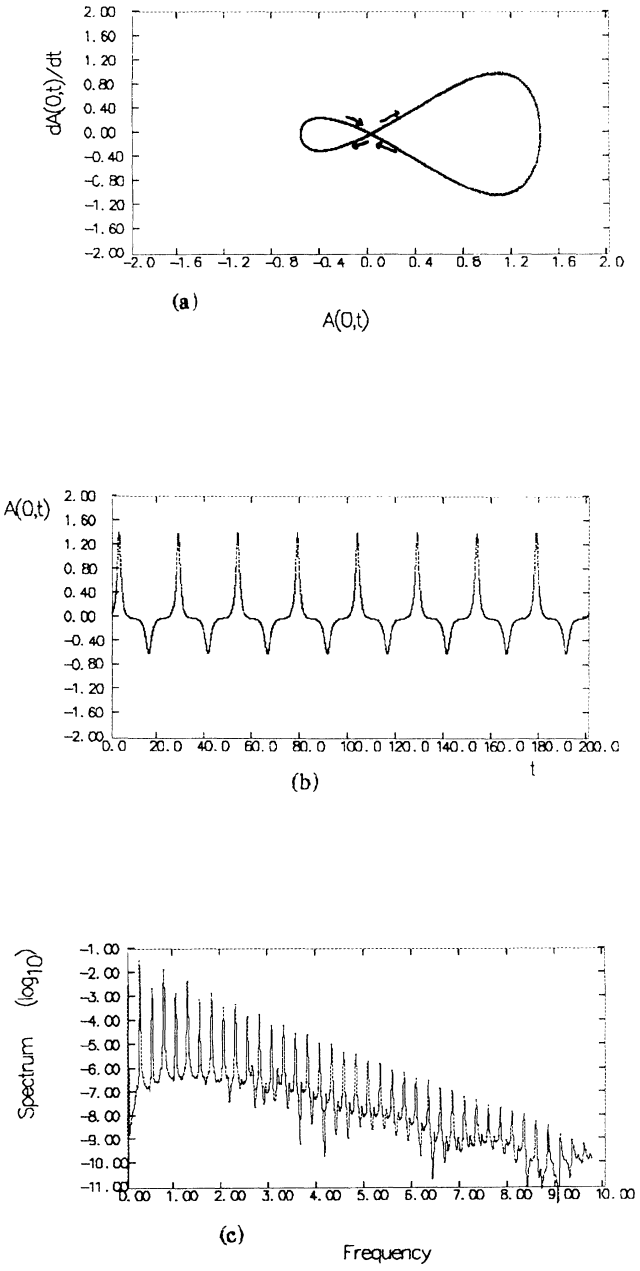

FIG. 3. Solution of Eq. (1) with $\theta=45.225°$. (a) Phase trajectories, where arrows indicate the directions of motion. (b) The time evolution of the amplitude of fields. (c) The Fourier spectrum of $A(0,t)$ with respect to time.

crossings have been observed. These demonstrate the presence of stochastic motions for complicated dynamics. The time evolutions for the amplitude of fields also exhibit the irregular motions, and the power spectra clearly indicate the broadband structures and noiselike spectra being typical of chaotic time evolutions. These phenomena show that the high-order Hamiltonian perturbation in Eq. (2) leads to chaos. As far as plasma turbulence is concerned, the cubic NSE describes the nonlinear interaction between the Langmuir wave and ion-acoustic wave under the subsonic regime, and finite soliton solutions can be obtained by IST. Solitons developed by parameteric instabilities keep their spatially coherent structures and temporally periodic evolutions. The velocity of field propagation remains constant [Fig. 6(c)]. In long-time evolution processes, integrability would be broken down by other physical effects, for example, damping, dissipation, and high-order nonlinearity. In this paper, our dynamic model shows that Langmuir wave fields are no longer periodic evolutions even without damping and dissipative effects, but still keep their spatially localized structures. Figures 4(d) and 5(d)

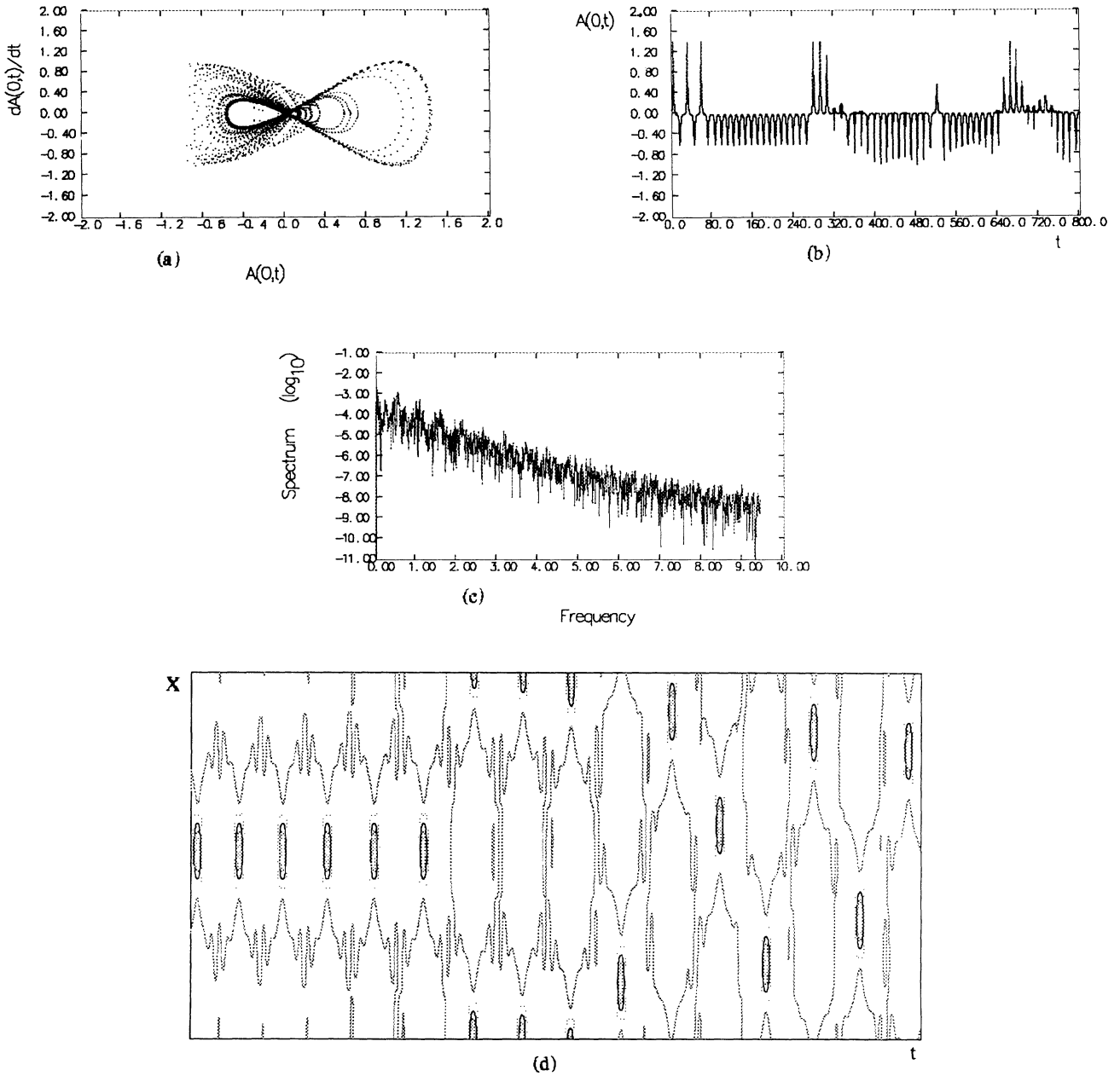

FIG. 4. Chaotic trajectories of Eq. (2) with $g=0.001$ and $\theta=45.225°$. (a) Phase motions in the phase space. Notice the irregular HMO crossings. (b) The time evolution of the amplitude of fields. (c) The Fourier spectrum of $A(0,t)$ indicates the broadband structure and noiselike spectrum being typical of chaotic time evolution. (d) Contours of $|E(X,t)|^2=$const, where $t=550-700$ and $X=-L/2\sim L/2$.

indicate that due to the high-order nonlinear effects the propagative velocity of the localized structures is not constant.

V. RECURRENCE AND STOCHASTICITY

In the Introduction, we simply accounted for the recurrence of the cubic NSE, which is associated with complete integrability. For Eq. (2), Cloot, Herbst, and Weideman [12] qualitatively proved the existence of bound solutions by use of the invariant (5) and (7). Their numerical results displayed the recurrence of solutions. Here, we further analyze the relationship between recurrence and stochasticity. For the initial condition (37), we expect that recurrence should easily appear nearby those trajectories corresponding to $\theta=90°$; Figure 7 illustrates the type of recurrence, where $g=0.2$ and $\theta=90°$. The phase orbit corresponds to a periodic motion of three-cycle, which can also be verified in Fig. 7(b) from the well-formed structures of the time evolution of field amplitude for long-time prediction. The FPU recurrence phenomenon is displayed in Fig. 7(c), where three kinds of spatially localized structures appear and the velocity of field propagation is invariable. Comparing Figs. 6 and 7, we observe that the recurrence period for $g=0$ is about five times as long as that for $g=0.2$.

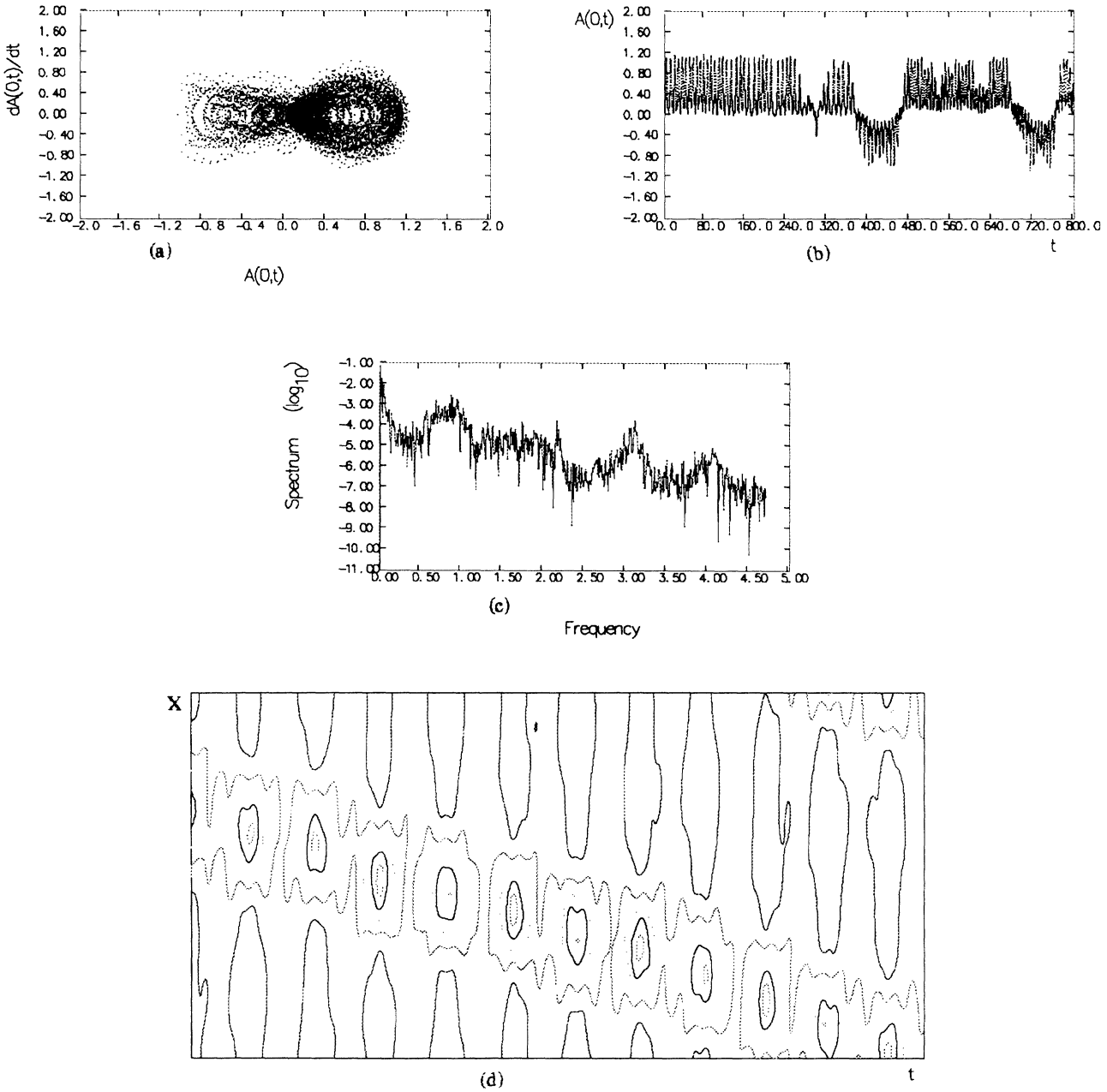

FIG. 5. Chaotic trajectories of Eq. (2) with $g=0.1$ and $\theta=45.225°$. (a), (b), and (c) as before, and (d) corresponds to $t=400-560$.

If we choose the different parametric values g and change the initial phase, we observe that the chaotic behavior appears as shown in Table I. These phenomena demonstrate that the recurrence sensitively depends on the initial conditions and the parametric values. The results in Table I express that the recurrence only is the special feature and the stochasticity should be the main one for the dynamic system (2). The fact that these completely different dynamic behaviors occur is very interesting and important. Obviously, the presence of recurrence is not necessarily associated with complete integrability. Our recent numerical investigations seem to indicate that there may be cases in which both effects, recurrence and

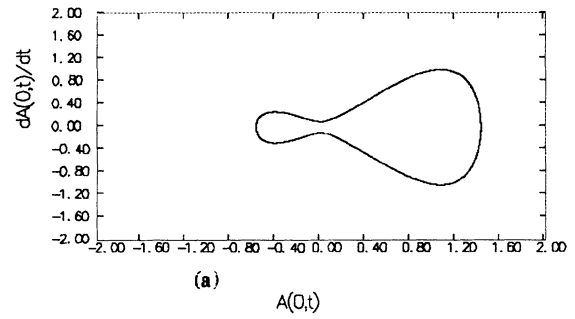

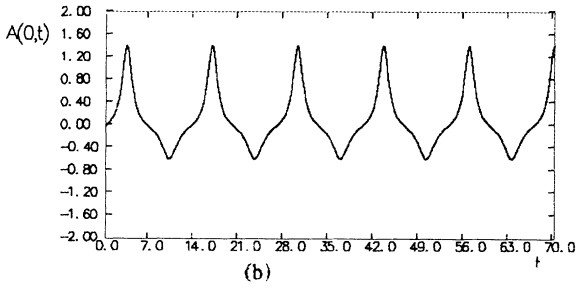

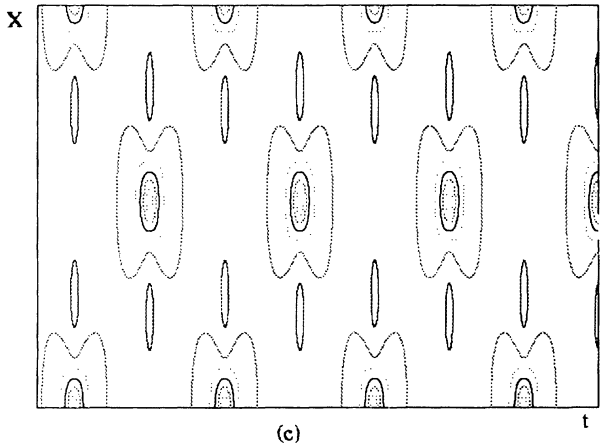

FIG. 6. solution of Eq. (1) with $\theta=90°$. (a) and (b) as illustrated in Fig. 3. (c) Contours of $|E(X,t)|^2=$const, where $t=0-50$.

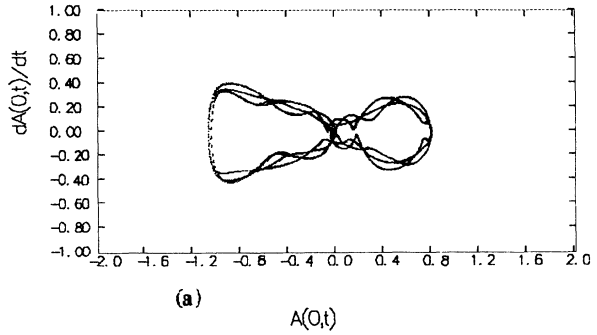

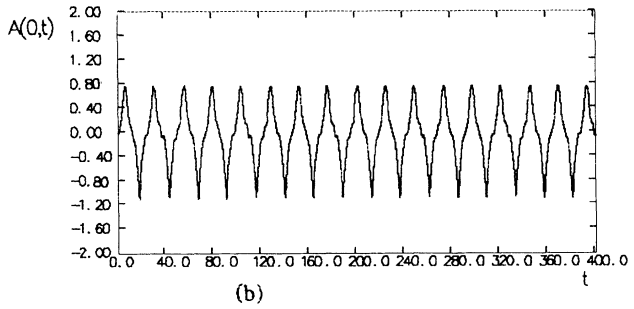

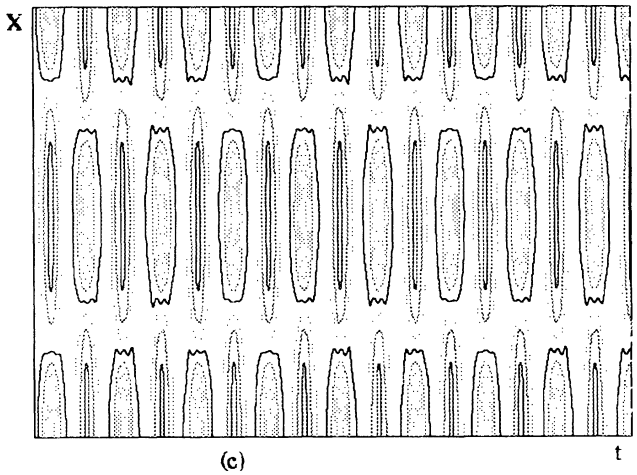

FIG. 7. Solution of Eq. (2) with $g=0.2$ and $\theta=90°$. (a), (b), and (c) as indicated in Figs. 6, where (c) corresponds to $t=0-200$. Note that the well-formed structures in (b) and (c) show that the period of recurrence is about five times as long as that in Figs. 6(b) and 6(c).

TABLE I. The letter C represents chaos and R represents recurrence. — shows that there is no numerical result.

g / θ (deg)	0.001	0.05	0.1	0.2	0.245	0.249
45	—	C	C	C	—	—
45.225	C	—	C	C	R	C
90	—	C	C	R	C	C

stochasticity, are simultaneously important for the dynamic system (2).

VI. CONCLUSIONS

A systematic analysis on the dynamic properties of high-order NSE (2) has been given. One of the most important conclusions is that the high-order Hamiltonian perturbation (i.e., quintic nonlinear effects) may lead to the breakdown of NSE integrability. For plasma physics, our dynamic model can be derived from Vlasov-Maxwell equations. The cubic NSE describes the nonlinear interaction between the Langmuir wave and the ion-acoustic wave in the subsonic regime, where the interaction of the second-order fields is only considered. In the initial stages of field evolutions, many physical phenomena, such as solitons developed by modulational stabilities, can be explained in terms of this model. In strong turbulent plasma theory, however, the cubic NSE is no longer valid. The other physical effects, for example, damping and dissipation, have to be considered. These effects would lead to stochasticity. In particular, the high-order field interaction has to be dealt with in the evolutive later stages of plasma instability. Although our dynamic model only involves the fourth-order field interaction, it is shown that this high-order Hamiltonian perturbation may also result in the presence of chaos. The field evolution from coherence to turbulence is temporally chaotic but keeps their spatially localized structures. The propagative velocity of the localized structures is variable where the mechanism is due to high-order nonlinear effects.

For a finite-dimensional dynamic system, of course, it is well known that small nonintegrable perturbations can lead to chaos [33]. Some important properties, such as a route to temporal chaos by double periodic bifurcation and irregular HMO crossings, etc, are also observed in the infinite-dimensional dissipative systems [18,30,34]. Our numerical results have also shown that the irregular HMO crossings occur in the presence of high-order Hamiltonian perturbation. Possible theoretical work on the HMO chaos may be continued in terms of Melnikov's method [34–36]. Owing to the complication consisting of a scattering spectrum for the cubic NSE with periodic boundary, however, it may be very tedious and difficult work.

On the other hand, a periodic solution and a solitary-wave solution have been obtained analytically. The parameteric values of periodic solutions can be given in virtue of pseudoenergy H_0. It is shown that the effects of high-order nonlinear terms enhance the amplitude and width of the solitary wave, and weaken the density depletion as compared with those for the cubic NSE. The recurrence solutions could be associated with a class of periodic solutions, but our results on recurrence do not correspond to our periodic solution. The reason is that the periodic solution in Sec. II is a traveling-wave solution, but the recurrence solution is derived from the initial-value problem with periodic boundary condition. Such a recurrence behavior which sensitively depends on the initial conditions is a general feature of Hamiltonian systems but is not necessarily associated with complete integrability.

It is worthwhile for us to analyze the detailed relationship between recurrence and stochasticity. In subsequent study, we expect that some theoretical work can be obtained. In addition, we plan to discuss some more interesting phenomena, for example, critical value g_c, energy spectrum, etc.

ACKNOWLEDGMENTS

We wish to acknowledge useful discussions with Professor B. L. Gou about the problem of the integrability of NSE, and we are grateful to S. P. Zhu for helping in numerical discussions. One of us (C.T.Z.) would like to thank Tan Yu for his stimulated discussions on various issues relating to this paper. This research has been supported by the National Natural Science Foundation of China, Grant No. 1880109.

[1] V. E. Zakharov and A. B. Shabat, Zh. Eksp. Teor. Fiz. **61**, 118 (1972) [Sov. Phys. JETP **34**, 62 (1972)].
[2] M. J. Ablowitz and J. F. Ledik, Stud. Appl. Math. **55**, 213 (1976).
[3] *Soliton*, edited by R. K. Bullough and P. J. Caudrey (Springer-Verlag, Berlin, 1980).
[4] T. B. Benjamin and J. E. Feir, J. Fluid. Mech. **27**, 417 (1967).
[5] A. Thyagaraja, Phys. Fluids **22**, 2093 (1979).
[6] A. Thyagaraja, Phys. Fluids **24**, 1972 (1981).
[7] E. Fermi, T. Pasta, and S. Ulam, *Collected Papers of Enrico Fermi*, edited by E. Segre (University of Chicago, Chicago, 1965), p. 978.
[8] B. M. Lake, H. C. Yuen, H. Rungaldier, and W. E. Ferguson, J. Fluid. Mech. **83**, 49 (1977).
[9] H. C. Yuen and B. M. Lake, Phys. Fluids **18**, 956 (1975).
[10] H. C. Yuen and W. E. Ferguson, Phys. Fluids **21**, 1275 (1978).
[11] M. Stiassnie and U. I. Kroszynski, J. Fluid. Mech. **116**, 207 (1982).
[12] A. Cloot, B. M. Herbst, and J. A. C. Weideman, J. Comput. Phys. **86**, 127 (1990).
[13] B. J. Lemesnrier, G. Papanicollaon, C. Sulem, and P. L. Sulem, Physica D **31**, 79 (1988).
[14] X. T. He, Acta Phys. **31**, 1317 (1982) (in Chinese).
[15] Z. J. Liu and X. T. He, Kexue Tong Bao. **29**, 1328 (1984).
[16] S. G. Thornhill and D. ter Haar, Phys. Rep. **43**, 79 (1978).
[17] M. S. Cramer and L. T. Watson, Phys. Fluids **27**, 821 (1984).
[18] T. H. Moon, Phys. Rev. Lett. **64**, 412 (1990).
[19] K. H. Spatschek, H. Pietsch, E. W. Leadk and Th. Erckermann, in *Nonlinear and Turbulent Processes in Physics,*

edited by V. E. Bar'yakhtar *et al.* (World Scientific, Singapore, 1989), Vol. 1, p. 10.
[20] K. Nozaki and N. Bekki, Phys. Rev. Lett. **50**, 1226 (1983); J. Phys. Soc. Jpn. **54**, 2363 (1985); Physica D **21**, 381 (1986).
[21] K. J. Blow and N. J. Doran, Phys. Rev. Lett. **52**, 526 (1984).
[22] K. H. Spatschek, H. Pietsch, E. W. Leadk, and Th. Erckermann, in *Singular Behavior and Nonlinear Dynamics,* edited by St. Pnevmatikos *et al.* (World Scientific, Singapore, 1989), Vol. 2, p. 555.
[23] T. H. Moon and M. V. Goldman, Phys. Rev. Lett. **53**, 1821 (1984).
[24] N. Nakhmediev, D. R. Heatley, G. I. Stegeman, and E. M. Wright, Phys. Rev. Lett. **65**, 1423 (1990).
[25] K. Nozaki and N. Bekki, Phys. Lett. **102A**, 383 (1984).
[26] W. Shyu, P. N. Guzdar, H. H. Chen, Y. C. Lee, and C. S. Liu, Phys. Lett. A **147**, 49 (1990).
[27] O. Larroche and D. Pesme, Phys. Fluids B **2**, 1751 (1990).
[28] A. B. Bishop, K. Fisser, P. S. Lomdahl, W. C. Kerr, M. B. Williams, and S. E. Trullinger, Phys. Rev. Lett. **50**, 1095 (1983).
[29] See also K. H. Spatshek, H. Pietsch, E. W. Leadke, and Th. Erckermann, in *Nonlinear and Turbulent Processes in Physics* (Ref. [19]), p. 978.
[30] F. Kh. Abudallaev, Phys. Rep. **179**, 1 (1989).
[31] K. Nozaki, Physics D **23**, 369 (1986).
[32] T. R. Taha and M. J. Ablowitz, J. Comput. Phys. **55**, 202 (1984).
[33] A. J. Lichtenberg and M. A. Lieberman, *Regular and Stochastic Motion* (Springer-Verlag, Berlin, 1984).
[34] M. Taki, K. H. Spatschek, J. C. Fernandez, R. Grauer, and G. Reinisch, Physica D **40**, 65 (1989).
[35] P. Holmes, in *Dynamical Systems and Turbulence, Warwick 1980,* edited by A. Dold and B. Echmann (Springer-Verlag, Berlin, 1981), p. 164.
[36] J. Cuckenheimer and P. Homles, *Nonlinear Oscillations, Dynamical Systems and Bifurcations of Vector Fields* (Springer-Verlag, Berlin, 1983).

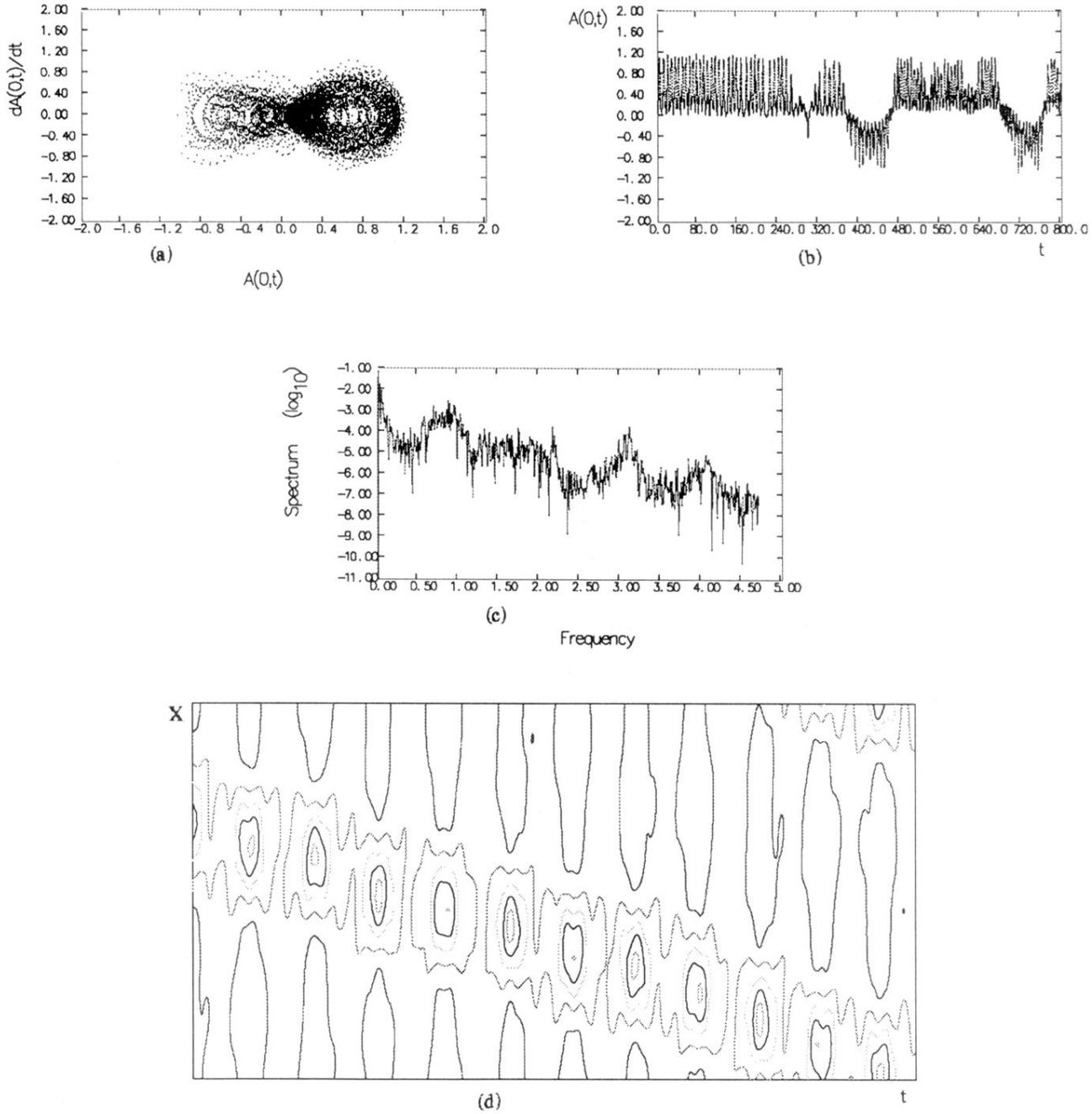

FIG. 5. Chaotic trajectories of Eq. (2) with $g=0.1$ and $\theta=45.225°$. (a), (b), and (c) as before, and (d) corresponds to $t=400-560$.